

**UKAEA FUS 412**

**EURATOM/UKAEA Fusion**

**A Nonlinear Dynamical Model of  
Relaxation Oscillations in Tokamaks**

A Thyagaraja, F A Haas, D J Harvey

December 1998

**© UKAEA**

EURATOM/UKAEA Fusion Association

Culham Science Centre, Abingdon  
Oxfordshire, OX14 3DB  
United Kingdom  
Telephone +44 1235 463449  
Facsimile +44 1235 463647



# A Nonlinear Dynamical Model of Relaxation Oscillations in Tokamaks

A. Thyagaraja, F.A. Haas\* and D.J. Harvey

EURATOM/UKAEA Fusion Association, Culham Science Centre, Abingdon, OX14 3DB,  
UK.

## Abstract

Tokamaks exhibit several types of relaxation oscillations such as sawteeth and Edge Localised Modes (ELMs) in H-mode. Several authors have introduced low dimensional (ie, systems with a small number of modes or degrees of freedom) nonlinear models which can illustrate the generic characteristics of such oscillations. In models of this kind, no attempt is made to simulate all the myriad details of the fundamentally nonlinear phenomena in question, but the focus is on physically 'relevant' degrees of freedom. These often involve the plasma macroscopic quantities such as pressure or density and also some measure of the plasma turbulence which is thought to control transport. In addition, 'coherent' modes may be involved in the dynamics of relaxation, as well as radial electric fields, sheared flows etc. In the present work we present a minimal extension of our earlier sawtooth model which effectively contained only two degrees of freedom. We have introduced additionally a pressure-driven 'coherent' mode which interacts with the turbulence in a specific manner. The price paid for this increased realism and generality is that the number of parameters which are involved in the dynamical specification of the model also increases. Holding all but two of them fixed, we have studied some of the bifurcation properties of the system. These turn out to be remarkably rich and varied and strongly suggestive of the behaviour found experimentally in actual tokamaks. More specifically, the present system with three degrees of freedom is the simplest known to us which can yield features reminiscent of sawteeth, compound sawteeth, intermittency, chaos, periodic and 'grassy' ELMing according to the choice of the control parameters and model interpretation. The main message of the model seems to be that linear instability behaviour of systems, while useful in elucidating 'drives' for instabilities, can be misleading in understanding the dynamics of nonlinear systems over time-scales much longer than linear growth times and states far from stable equilibria.

December 1998

\* Oxford Research Unit, The Open University, Boars Hill, Oxford.

PACS numbers: 05.45.+b, 52.35.Ra, 52.55.Fa, 53.35.Py

## 1. Introduction

The purpose of the present paper is to consider qualitatively, by means of a physically motivated extension of a previously developed nonlinear model, some of the *generic* features of two basic relaxation phenomena found in tokamaks: namely sawteeth and Edge Localised Modes (ELMs). In earlier papers<sup>1-4</sup> we had developed a version of the model which effectively had only two degrees of freedom and which we then applied to experimental situations. Our aim in the present work is rather different: firstly we seek to consider more explicitly, the possible influence of a ‘coherent mode’ on the system dynamics. Such a mode is known to exist in the sawtooth case, but is not always seen as a ‘precursor’ to the crash. The crash generally involves a *thermal energy* redistribution within the core, but not necessarily a *magnetic* one (ie most modern tokamaks exhibit partial reconnection, whenever an attempt is made to measure the  $q$ -profile within the core). It is one of the outstanding problems of sawtooth dynamics to understand in detail how partial reconnection of the magnetic flux can be compatible with a temperature or  $\beta$  crash.

Our second aim is to study the bifurcation properties of the model and consider such questions as: is dynamic stabilization of relaxation phenomena possible? Can simple models exhibit ‘subcritical’ bifurcations or ‘metastable’ behaviour? As we demonstrate by means of numerical solutions to the present model, answers to both questions is a qualified ‘yes’. It was an unexpected outcome of the model that some solutions exhibit ‘bursty’ chaos and ‘long time memory’ related to ‘monster sawteeth’. The model also demonstrates that it may be possible to dynamically stabilize (as suggested by us<sup>5</sup> in the case of the  $m = 1$  resistive internal kink) at least some of the large-scale relaxation oscillations. The chaotic solutions tend to become periodic under the influence of external perturbations of a simple form and relatively small amplitude. Another key conclusion one can draw from the examples presented is the fact that a linear ‘trigger’ is not necessarily involved in crashes. The system, in effect, has memory and this is sufficient for periodic, ‘double periodic’, quasi periodic and chaotic behaviour. On the other hand, linear theory does appear to provide valuable guidance on the kinds of drive necessary for relaxation oscillations to occur and in determining regions of parameter space where transitions are likely to occur between steady and periodic states of the system.

Apart from the papers by us on the sawteeth cited above, several authors have proposed semi-quantitative dynamical models of relaxation phenomena (fishbones<sup>6</sup>, L-H transitions<sup>7, 8</sup>, ELMs<sup>9, 10</sup>) in tokamaks. Typically these low dimensional models are based on a small number of dynamical variables (ie functions of time) which satisfy coupled nonlinear equations of motion. The latter are sometimes derived from the full set of plasma equations (fluid or kinetic) after the introduction of certain simplifying assumptions. The idea is to capture the essence of the qualitative properties of the real system in a model which is simple enough to understand. The analytical and computational tools which are required for this purpose often turn out to be impractical in the case of the real system due to the very large number of degrees of freedom typical of such systems. Often, one uses physical arguments to derive the equations governing these ‘reduced’ model systems. The constants (ie system parameters) in the relevant equations are related to discharge and machine properties through the medium of standard equilibrium and stability theories. The models, although grossly simplified, are supposed to provide physically understandable paradigms which enable one to reach



qualitative understanding of the rather complicated, but hopefully *generic* aspects of the dynamics involved in actual experiments. The models also provide markers for more complete numerical simulations involving the full set of plasma fluid/kinetic equations. Although, in principle, the latter remain the most *general* method of theoretical investigation of relaxation phenomena, they are subject to many limitations and resource constraints which are unlikely to be overcome in the near future. It has been noted by several authors (eg. Diamond and co-workers<sup>8</sup> and by us) active in this field that, in analogy with condensed matter physics and ecology, reduced models such as ‘Ginzburg-Landau theory’ or ‘predator-prey’ population dynamics are very useful in bridging the rather large gap between strictly phenomenological descriptions of experiments and ‘microscopic’ theories based on complete equations of motion.

In earlier investigations<sup>1, 2, 3</sup> we attempted to construct a picture of sawtooth dynamics based on a two degree-of-freedom model, taking account of both turbulence and transport. Although the  $m = 1$  mode was present in the background turbulence, it did not play the central role required of it in the more conventional approach of Aydemir *et al*<sup>11</sup>, for example. In the present paper we further develop our model to include the interaction between a ‘pressure-driven’ coherent mode and the turbulence. This more general study results in a three degree-of-freedom system and is relevant, with suitable interpretation of the dynamical variables and control parameters, to both sawteeth and ELMs. It is, nevertheless, considerably simpler than the full-scale numerical simulation of the complete tokamak plasma dynamics. It is generally accepted that microinstabilities can enhance or damp coherent modes, depending upon the conditions. Equally, single, coherent modes can easily give rise to ‘secondary microinstabilities’ which can alter the transport properties of the system drastically. It is also well-known<sup>12</sup> that three or more degrees of freedom can lead to quite new qualitative effects such as ‘chaotic’ behaviour, as opposed to periodic solutions characteristic of two degree-of-freedom systems. The model presented below is not intended to be a systematic approximation to the full set of equations, and as such, we do not attempt a rigorous derivation. However, physical arguments will be advanced to motivate the formulation of the mathematical model.

The material presented is laid out as follows: in the next Section, we take our sawtooth model of the earlier papers and develop it further as described above to include the dynamics of a coherent mode. This mathematical formulation is supplemented by the physical ideas on which it is based. In Section 3, the analytical results relating to steady states and linear stability of such stationary solutions are given. Section 4 describes the rather diverse ‘zoology’ of the solutions of the system of three nonlinear differential equations as certain system parameters are varied. In particular, we discuss the bifurcation properties of the system as the growth rate and nonlinear saturation characteristic are varied. The concept of ‘coexistence’ or metastability of the system is introduced and the regions where chaos, quasiperiodicity and intermittency with ‘monster’ sawtoothing occurs are discussed. In Section 5, we abstract the generic properties of the system and suggest that the dynamical equations, with suitable reinterpretation, may be applicable to ELM physics. Experimentally, ELM characteristics often present a remarkable formal similarity to sawteeth wave forms, and theoretically this may be a reflection of similar dynamical mechanisms in both sets of phenomena. We also present a brief discussion of the relation between our approach and two recent works<sup>8, 10</sup> which are based on rather different physics but share a philosophy similar to the present

work. Our conclusions are presented in Section 6.

## 2. Description of the model

The model involves the dynamical interaction of three functions of time. These relate to suitable integrals over space of appropriate variables (eg. plasma pressure). Of the first two,  $Z(t)$  is a nondimensional measure of the pressure, and  $W(t)$  is taken to be a dimensionless measure of the turbulence intensity. In the present model we do not distinguish between electrostatic and electromagnetic turbulence, although this could always be done by introducing separate electrostatic and magnetic turbulence levels<sup>8</sup>. However, this would increase the number of degrees of freedom by at least one. In principle,  $W$  stands for both effects, although in the ‘sawtooth’ interpretation and possibly also the ELM interpretation, it more nearly represents magnetic fluctuation levels. The third function of time,  $X(t)$  is a nondimensional measure of ‘coherent mode’ activity. For example,  $X$  could represent the  $m = 1$  island width. We first consider the sawtooth model in the following discussion.

In the equations which follow, all variables and parameters, except the time,  $t$ , and  $\tau_s$  will be dimensionless; as in our earlier papers<sup>2,3</sup>,  $\tau_s$  is a typical energy confinement time appropriate to the problem.

Guided by our earlier work<sup>2,3</sup> we take the three variables mentioned, to satisfy the following system of nonlinear ordinary differential equations:

$$\tau_s \frac{dZ}{dt} = 1 - \Gamma_Z(W)Z \quad (1)$$

$$\tau_s \frac{dW}{dt} = \Gamma_W(Z, W, X)W \quad (2)$$

$$\tau_s \frac{dX}{dt} = \Gamma_X(Z, W, X)X \quad (3)$$

In the above equations, the nonlinear rate functions,  $\Gamma_{Z,W,X}$  are assumed to take the forms,

$$\Gamma_Z(W) = (W + \kappa) \quad (4)$$

$$\Gamma_W(Z, W, X) = [\Phi(W)\Lambda(Z - 1) + 2(X - X_c)(\Gamma_Z(W)Z - 1)] \quad (5)$$

$$\Phi(W) = \frac{2W}{1 + W} + \kappa \quad (6)$$

$$\Gamma_X(Z, W, X) = \gamma[(Z - Z_c) - \alpha X \Gamma_Z(W)] \quad (7)$$

We note that these forms do not include explicit time dependence (ie the system is autonomous) or show singular behaviour, and are, apart from the  $\phi(W)$  function, polynomials of at most third degree. In particular, they do not contain Heaviside functions as ‘triggers’. These properties are qualitatively similar to the structure of the evolution equations of a tokamak plasma with constant sources and boundary conditions. From our earlier papers it is clear that this model *assumes* partial reconnection at the sawtooth crash and takes from experiment the fact that the  $q = 1$  radius is hardly affected by the crash. Thus it describes thermal redistribution within the  $q < 1$  zone in terms of anomalous transport triggered by the crash, but the current redistribution (in principle describable by the induction equation) is never complete (ie the  $q$  profile is only slightly affected by the sawtooth).

From the structure of these equations, it is clear that Eqs.(1-3) imply that  $Z, W$ , and  $X$  can always be chosen to be positive, and cannot change their sign. Equation(1) has an



inhomogeneous ‘source term’, which is normalized to unity. This implies that  $\kappa$  is a measure of nonturbulent losses relative to the ‘drive’, or source. As it stands, the model involves six nondimensional control parameters,  $\kappa, \Lambda, X_c, Z_c, \gamma$  and  $\alpha$ . We have already noted that  $\tau_s$  is a characteristic time involved in the problem. It can of course be eliminated by an appropriate re-scaling of time, setting for example,  $t = \tau_s u$ , where  $u$  is a dimensionless ‘time’ variable.

The physical interpretation and the provenance of these equations will now be given. The equation for  $Z$ , ie Eq.(1) has already been derived in this form in our earlier papers<sup>2,3</sup>. In these papers, it was assumed that the change in pressure (represented by  $Z - 1$ ) due to the dynamics was small compared to its time-average value (normalized to unity), and the turbulent loss was assumed to be linearly proportional to the normalized turbulence level,  $W$ . In the present paper, we allow for large changes in the pressure (to describe ‘monster sawteeth’, ‘giant ELMs’ etc) by making the turbulent loss term,  $-WZ$ , rather than  $-W$ . All other ‘nonturbulent losses’ such as neoclassical and radiative are modelled by  $-\kappa Z$ , where  $\kappa$  is a suitable constant. We note that the present model reduces to the previous one in the limit,  $|Z - 1|, \kappa \ll 1$ .

Equation(1) then represents the change in the plasma stored energy due to heating (represented by the normalized source term), taking into account the turbulence-dependent losses (the  $WZ$  term) and any residual losses (due to neoclassical and/or radiation effects) represented by the  $\kappa Z$  term. The model is highly simplified in that the residual (ie ‘non turbulent’) losses are crudely represented by a simple ‘relaxation time’ approximation. The parameter  $\kappa$  is expected to be a number lying between zero and unity in problems of interest, although larger values may be appropriate in certain conditions. This change in form of the turbulent losses (relative to our original model) has an important qualitative effect: even in the absence of the  $\kappa$  term and the terms in the  $W$  equation coupling all three dynamical variables, the present model does not have a constant of the motion, unlike our earlier one, and is fundamentally irreversible. In this sense, the present model is more ‘generic’ of driven dissipative systems than the previous model which, in a limit, led to exactly integrable, periodic solutions.

We note that the coherent mode amplitude (eg. island width),  $X$ , does not enter this energy ‘balance’ equation directly. The transport due to the coherent mode is indirect in our model. Thus any losses are mediated directly by the turbulence  $W$ , which will, itself, generally be affected by the presence or otherwise of the coherent mode.

We next turn to Eq.(3), which governs the temporal evolution of the coherent mode. We have chosen a ‘Landau-Stuart’ type model equation of virtually definitive simplicity to represent the physics. In the absence of turbulence (ie, when  $W \equiv 0$ ) and in the linear limit, ( $X \ll 1$ ), observe that  $\Gamma_X \simeq \gamma(Z - Z_c)$ . This says in effect that if  $\gamma > 0$ , and  $Z$  exceeds a certain ‘threshold value’,  $Z_c$ , the mode is driven unstable by pressure (for example, a mechanism of this kind was proposed by Bussac *et al*<sup>13</sup>). This fact suggests that this is a generic feature of all temperature-gradient (eg. ion/electron temperature gradient modes) or pressure driven modes (eg. interchange, neoclassical tearing or ballooning modes). It should, in principle, be possible to extract suitable expressions for  $\gamma, Z_c$  from analytic (linear or nonlinear) stability theory. It is clear that the actual ‘linear’ growth rate is  $\gamma(Z - Z_c)/\tau_s$ . The interpretation of the second term of  $\Gamma_X$  is now straight forward: It is a nonlinear saturation effect, frequently encountered in tearing mode theory and elsewhere. The constant  $\alpha$  measures the strength of this saturation term. The smaller the value of  $\alpha$ ,



the larger the saturation amplitude of the mode. Note that if  $\alpha < 0$ , we have a case of nonlinear amplification of the linear instability (as might happen with major disruptions). In such cases the whole model breaks down and recourse must be had to the full equations of motion. We note that the form of the saturation term embodies the following intuitive idea: it is envisaged that strong turbulence would have a *damping* effect on the coherent mode, since nonlinear coupling of a linearly unstable mode to a ‘sea’ of stable modes of the plasma would tend to reduce its growth by a form of nonlinear radiation damping. We note that it is also possible to interpret this term as representing turbulence-driven  $\mathbf{E} \times \mathbf{B}$  flow shear damping. In this interpretation, the flow is assumed to be self-consistently generated by  $W$  (via the sum of Reynolds stresses and neoclassical effects, and is hence assumed proportional to  $W + \kappa$ ). This completes the motivation for the choice of  $\Gamma_X$ . At no point do we introduce explicit ‘trigger’ effects involving Heaviside functions which discontinuously affect the dynamical evolution, as done by certain authors<sup>9</sup>.

Finally we discuss Eq.(2) which governs the time evolution of  $W$ . Firstly, we note the close resemblance of  $\Gamma_W$  to the corresponding function in our earlier works<sup>2, 3</sup>. We envisage  $\Lambda$  to be a large number, say  $\geq 100$ , representing the fast growth rate of the microscopic modes which constitute  $W$ , relative to the ‘slow’ time-scale represented by  $\tau_s$ . However, the growth and decay of the turbulence are related to the turbulence level itself, as explained in earlier works. Thus, we have here a *nonlinear instability* of the turbulence driven by the pressure excess above threshold (ie  $Z > 1$ ) which achieves the full linear growth rate,  $\Lambda/\tau_s$ , only for large turbulence levels. This means that small levels of turbulence tend to reduce growth rates to below the levels predicted by linear theories. This again is an instance of nonlinear effects tending to ‘ameliorate’ linear instabilities, in this instance, at small turbulence levels.

In the sawtooth interpretation of the equations,  $\Lambda$  is related to the ratio of the sawtooth period to the crash time. The first term is exactly what we had used earlier. The provenance of the second term, proportional to  $-\tau_s(X - X_c)\frac{dZ}{dt}$  is more subtle. Qualitatively, this term describes the fact that as the coherent mode rises above a certain threshold amplitude  $X_c$ , it can drive ‘secondary instabilities’ which grow from it. This is analogous to the generation of modulational or parametric instability familiar in plasma theory and elsewhere. The form we have chosen is possibly the simplest, given the basic requirement that the model resemble our earlier model as much as possible. A key feature of this second, coupling term is that, for  $X > X_c$ , the factor multiplying it is directly proportional to the heat flux *out* of the system (ie to  $-\frac{dZ}{dt}$ ). The significance of this in the ELM interpretation of the model is that it is actually a mathematical embodiment of a ‘heat flux-driven’ instability. When the pressure is falling, the heat-flux to the plasma edge can cause extra recycling which drives certain linear modes unstable. Thus when the coherent mode amplitude is above threshold, rising pressures (at constant heating rate, this means that the heat-flux to the boundary is reducing) have a stabilising effect on the turbulence through this term, whilst falling pressure adds to the growth of  $W$ . In effect this term describes the transformation of internal energy (or pressure gradient) to turbulence and vice versa. Note also that unless  $Z \simeq 1$ , this term is always small compared with the first term, except at ‘crashes’ when the time rate of change of  $Z$  can be high, or  $X$  is particularly large.

We had shown<sup>3</sup> that the second term can be formally derived, at least in part, from the equations of motion by making certain moment closure approximations. In fact, although we shall not give the argument here, following a detailed extension of our earlier model, it

is possible to derive the  $-\tau_s \frac{dZ}{dt}$  form of the second term without making moment closure approximations. It turns out that Lenz' law (ie, the induction equation) is responsible for the form taken by this term. However, neither of these derivations leads to the  $(X - X_c)$  factor which is crucial to describe the interaction with the coherent mode. The inclusion of this factor is essentially postulated here rather than derived from the complete dynamical equations of the plasma. It is this factor which is truly specific to the model, and makes it similar to semi-phenomenological, 'predator-prey' or 'Ginzburg-Landau' models which are not strictly derived from microscopic equations of motion.

### 3. Steady states and linear stability properties

Having described the rationale and principal structural features of our three equation model for relaxation oscillations, we turn to a discussion of some of the simplest properties. It is evident from the equations that there are essentially two sets of steady solutions. Thus,  $W = 0, Z = 1/\kappa$  together with  $X = 0$  or  $X = X_H = \frac{Z-Z_c}{\alpha(W+\kappa)}$  gives one set. The second set has,  $Z = 1, W = 1 - \kappa$  and  $X = 0$  or  $X = \frac{Z-Z_c}{\alpha}$ . All of these solutions may not be realized, since we require, on physical grounds, that the three dynamical variables must be nonnegative.

Consider the solution,  $W = X = 0; Z = 1/\kappa$ . This is a 'neoclassical' or 'turbulence-free' state in which there is no coherent mode activity. It may correspond to a sawtooth-free discharge. Suppose that  $\kappa, Z_c$  satisfy,  $Z = 1/\kappa < Z_c < 1$  for arbitrary, positive  $\Lambda, \gamma, \alpha, X_c$ . It is obvious from simple inspection that the solution is linearly stable. Numerical calculations also support this conclusion. When  $\kappa < 1$ , it is elementary to show that this solution must necessarily be linearly unstable, whatever the value of  $X, \Lambda, \gamma, X_c Z_c$ .

Another steady solution is obtained by setting  $Z = 1, W = 1 - \kappa$ . This can only exist (since we require  $W > 0$  on physical grounds) if  $\kappa < 1$ . There are two possibilities: either,  $X = 0$  or  $X = (1 - Z_c)/\alpha$ . If  $Z_c > 1$ , the second solution is impermissible, but  $X = 0$  is allowed. If  $Z_c < 1$ , both solutions are allowed, but it is easily seen that  $X = 0$  is linearly unstable. Let us therefore consider this case. Assuming  $\Lambda \gg 1$ , a relatively simple linear analysis of the full set of equations about this steady solution is easy to carry out. This shows that the steady state with,  $Z = 1, W = 1 - \kappa, X = (1 - Z_c)/\alpha$  is stable provided  $(1 - Z_c)/\alpha - X_c < \frac{1}{2(1-\kappa)}$ . If  $\alpha$  is sufficiently small (ie when,  $\alpha < \frac{1-Z_c}{X_c + \frac{1}{2(1-\kappa)}}$ ) this steady solution then becomes unstable and gives rise to periodic 'limit cycle' oscillations, characteristic of a Hopf bifurcation. Note that the criterion is independent of  $\Lambda, \gamma, \tau_s$ . This completes the enumeration of the steady solutions of the system and their linear stability properties. It is not hard to show that the dynamical variables cannot grow unboundedly (this is called 'Lagrange stability') in time. Furthermore, if the second, coupling term in the  $W$  equation is removed and  $\kappa = 0$ , the quantities  $W, Z$  satisfy a conservative system which can be explicitly integrated in terms of elliptic functions<sup>2</sup>.

### 4. Numerical simulations and classification of dynamical behaviour



It turns out that very little more can be learned about the model using purely analytical methods. For example, to discuss even the linear stability of the periodic solutions which arise from the steady ones through a standard Hopf bifurcation, one must have analytical forms of the solution to apply Floquet theory. Unfortunately, no such forms are known. For this reason, we consider the solutions of the initial value problem purely numerically. By taking a sufficiently small time-step and using a semi-implicit scheme (deliberately chosen to be similar to those employed in large-scale numerical simulations of tokamak turbulence to mirror their properties), we time-evolve the equations of motion with chosen sets of parameters and specified initial conditions.

We begin by considering the analytically predicted Hopf bifurcation. It turns out that the most interesting transitions occur in the  $\alpha, \gamma$  space when all other parameters are kept fixed. For definiteness, the following values were assigned to the ‘fixed’ parameters:  $\tau_s = 25\text{ms}$ ,  $\Lambda = 100.0$ ,  $\kappa = 0.1$ ,  $X_c = 0.1$ ,  $Z_c = 0.25$ . The transition from steady to periodic solution takes place at  $\alpha = 1.14$ . We show solutions in this  $\alpha, \gamma$  plane in a log-log plot (Fig.1). Essentially it is a bifurcation diagram of the system. This shows several remarkable features which will be described.

The most interesting (and unexpected) fact about this transition between stationary and periodic behaviour is the following. According to linear theory, at  $\alpha = \alpha_c \equiv \frac{1-Z_c}{X_c + \frac{1}{2(1-\kappa)}}$ , the steady solution bifurcates to a periodic limit cycle. Remarkably, we observe that the system appears to be ‘metastable’ at this transition. This is most clearly seen for  $\gamma = 10$ .

Thus, when the system is started off with initial conditions very close to the stationary solution, whenever  $\alpha$  exceeds the ‘critical’ value,  $\alpha_c$ , we find the solution is ‘attracted’ to the stable stationary solution. However, for initial conditions which are ‘far’ from this state, the system evolves into a finite amplitude, periodic solution! Thus, the system evolution is partly determined by the initial conditions and both the stationary and the periodic solutions ‘coexist’ in some neighbourhood of the ‘critical’ value for  $\alpha$  (the reader will recall from the analysis of the previous section, the transition is independent of  $\gamma$ ).

For  $\gamma = 10$ , Fig.1 shows that as long as  $\alpha$  does not exceed a *second critical value* of 2.9, there is a ‘coexistence region’ where we obtain both the periodic solution and the stationary one depending on the initial conditions. Figure 2a shows the three-dimensional ‘phase portrait’ (in  $Z-1, \log W, X$  space) of the trajectory of the system, starting with initial conditions:  $Z_0 = 1.05, W_0 = 0.9, X_0 = 0.6$ . In these simulations we have taken the time-step  $\Delta t = 1.25 \times 10^{-6}$ . The final epoch is 2.4 secs.

It is clearly seen that the trajectory spirals into the fixed point. Keeping all the system parameters exactly at these values but changing the initial conditions to  $Z_0 = 5.0, W_0 = 0.1, X_0 = 0.6$ , we obtain the periodic solution, as illustrated in Fig.2b. The three-dimensional ‘limit cycle’ is pictured in this diagram whilst the function  $Z(t)$  is given in Fig.2c. It is evident that this finite amplitude ‘sawtooth oscillation’ is very different from the stationary solution and yet, equally stable (ie numerically computable).

To demonstrate the stability of this periodic solution to small amplitude, externally imposed perturbations, a finite amplitude ‘noise’ or perturbation term of the form,  $W^{1/2}a \cos(\omega t)$  was added to the  $W$  equation with  $a = 1.0 \times 10^{-2}, \omega = 3/\tau_s$ . The solution was found to be unaffected by this level of externally imposed perturbation. At larger amplitudes, the solution is affected but its qualitative feature of periodicity is preserved.

This metastability or simultaneous coexistence of a periodic and steady solution for the



same set of system parameters is of considerable conceptual importance. It demonstrates a fundamental limitation of linearized stability analyses of complex nonlinear systems such as tokamak plasmas or fluids. For example, although the laminar flow in a pipe may be *linearly stable* to small amplitude perturbations at *arbitrary* Reynolds numbers, above an experimentally well-defined ‘critical Reynolds number’ the system may exhibit turbulence. In the present case, a linearly stable steady solution and a *periodic* solution (though not a turbulent one as in fluid mechanics) are shown to coexist at the same parameter values. Such behaviour, has not previously been reported (to the best of our knowledge) in low dimensional dynamical models systems such as ours. This type of metastability can, under appropriate circumstances, lead to hysteresis as the parameters  $\alpha$  and  $\gamma$  are varied on longer time-scales than the typical period of the system (due possibly to the sources imposed on the system varying in time).

The next type of bifurcation exhibited by the system is found when, for fixed  $\gamma$ , one lowers  $\alpha$ . At a value of  $\alpha < \alpha_c$  ( $= 1.14$  in our case), the system acquires ‘double periodicity’. This is illustrated by Figs.3a,3b. In a rather narrow range of parameters, this periodic solution appears to bifurcate into a ‘quasi-periodic’ one with two independent periods. An example is shown in Figs.4a,4b. In fact, this type of solution is difficult to readily distinguish from the ‘chaotic’ solutions, and only a few examples have been found. This suggests that the region in the parameter space where such solutions are found is rather small.

As we noted earlier, the key feature which distinguishes autonomous systems with three or more degrees of freedom from those with only two is the possibility of chaotic solutions. We have indeed found chaotic solutions (as indicated in Fig.1) for a variety of parameter values. For example, Figs.5a,5b,5c illustrate the solution obtained for  $\alpha = 0.25, \gamma = 0.5$ . The sharp ‘corners’ in the three dimensional phase portrait (Fig.5c) are an artefact of insufficient *graphical* resolution of the ‘crashes’, not actual numerical simulation errors. This is because the time-step of  $0.125\mu s$  is easily able to resolve the crash, but the time between successive plotted points is of the order of a millisecond.

In Figs.5d,5e we plot the frequency power spectrum of  $X$  in the chaotic case and a ‘periodic’ case  $\alpha = 0.8, \gamma = 0.5$  for comparison. As might be expected, chaotic spectra have a broad band decaying at high frequencies like an inverse power of the frequency in addition to sharp ‘line spectra’ indicating coherent components. The purely periodic solutions have mainly sharp lines at the harmonics of the fundamental sawtooth frequency. In the chaotic solutions, it is interesting to note ‘frequency chirping’ effects in the neighbourhood of crashes.

We have studied the effects of externally imposed periodic perturbations on the chaotic solutions. As an illustrative example, Figs.6a,6b show the ‘dynamic stabilization’ of the chaotic solution presented above when an external perturbation of the form,  $F_{ext} = \epsilon W^{1/2} \cos(\omega t)$ ;  $\epsilon = 0.1, \omega = 3/\tau_s$  was applied. It is seen that the solution is very similar to the ‘double periodic’ case. It is remarkable that this periodic solution which bifurcates into the chaotic one can be ‘reconstructed’ in this way by applying an external perturbation, which itself is not significant except at very small turbulence amplitudes. The latter fact can be seen by comparing the external perturbation with  $\Delta W$ , for example.

Keeping  $\gamma = 0.5$ , if we lower  $\alpha$  to  $0.2$ , we find ‘bursty chaos’. This type of highly irregular intermittent solution is illustrated in Figs.7a,b. The rather large coherent mode excursions are notable in these states.

As  $\gamma$  increases, we observe solutions which have qualitative features of the so-called



‘monster’ sawteeth. Thus, for  $\alpha = 0.2, \gamma = 1$ , we find solutions plotted in Figs.8a,b,c. A curious feature of this type of solution is the fact that the ‘pressure’,  $Z$ , attempts to rise to the steady state,  $Z = 1/\kappa$  during a period when there is very little turbulence, but rather large and rising values of  $X$  exist. As the linear theory shows, this state is unstable, and the evolution is always terminated by a crash when a very substantial degradation of plasma pressure takes place. The coherent mode is virtually totally suppressed for a while. The sawtooth exhibits both precursors and, interestingly, ‘postcursors’. The crashes appear to follow a random pattern. The power spectrum of  $X$  shows the ‘ $1/f$ ’ type behaviour, illustrative of the concentration of power at the lowest frequencies.

It is interesting to note that these ‘monsters’ can also be ‘tamed’ by dynamic stabilization. As before, when we include a periodic perturbation:  $F_{ext} = \epsilon W^{1/2} \cos(\omega t)$ ,  $\epsilon = 5.0, \omega = 3/\tau_s$ , we find that the solution becomes nearly periodic with relatively short period and low amplitudes. The results are shown in Figs.9a,b,c. The power spectrum shows that the power at  $3/\tau_s = 120\text{Hz}$ . is relatively small compared with the oscillation amplitudes of the sawtooth.

This completes the description of the ‘zoology’ of this system. It should be emphasised that we have by no means explored all parts of the parameter space. We have, however, considered the case when  $\phi \equiv 1$ , corresponding to purely linear growth of turbulence in the  $W$  equation. A very similar bifurcation diagram is obtained with the difference that the ‘metastability’ of the periodic solution appears to be absent.

## 5. Alternative interpretation of the model: ELM dynamics

Edge Localized Modes (ELMs) are of great importance in H-mode tokamak physics since they provide the means to exhaust impurities and helium ash, and help to keep the edge plasma density stable. A recent survey with references can be found in the review by Connor<sup>14</sup>. It is believed that large ELMs (‘giant’ or Type I) may place unacceptable thermal loads on divertors and other edge components. On the other hand, continuous small ELMs may be beneficial to a power plant. Much effort has gone into understanding the root causes of L-H transitions, ELMs and phenomena associated with them. It is probable that ideal MHD pressure -driven (‘ballooning’) and/or current-driven (‘peeling’) modes are responsible for ELMs. It is also likely that radial electric fields and flow shear associated with them play a role in stabilizing ELMs.

In the present work, we take a qualitative approach and consider the ELM phenomenon as a type of relaxation oscillation due to the coupling of pressure (or its radial gradient; the model does not differentiate between them), electromagnetic turbulence, and a large scale, MHD ‘coherent’ mode. In H mode, when the turbulence is low, the pressure profile at the edge steepens, and drives both the coherent and the turbulent fluctuations of the magnetic field. The latter increases the transport and serves to bring down the gradient, but due to nonlinearity, there is overshoot and one obtains either a limit cycle or chaotic oscillations. The model deliberately avoids the explicit introduction of radial electric field effects and electrostatic fluctuations, not because they are unimportant, but simply to keep the conceptual structure simple and the number of free parameters as minimal as possible. It shows that given the form of anomalous transport and any pressure or temperature gradient-

driven instability mechanism, a relatively simple set of equations can qualitatively reproduce a variety of properties of ELMs. Of particular interest are the ‘chaotic’ solutions and the fact that they may be stabilizable by suitable external perturbations. The model makes the qualitative prediction that such dynamic perturbations could, in suitable conditions, ameliorate the effects due to large ELMs and may be employable using various heating and/or momentum sources.

We now relate our work to two previously published papers<sup>10, 8</sup>, which are closest in spirit to that of our own. Taking them in turn, we compare and contrast their salient features and results with those of the present investigation. In order to study the dynamics of the L to H transition, Sugama and Horton<sup>10</sup> set up a model consisting of three coupled ordinary differential equations. The model is obtained for the resistive pressure-gradient driven turbulence and describes the evolution of three characteristic variables, namely, the potential energy contained in the pressure gradient, the turbulent kinetic energy and the shear flow energy. The energy input to the plasma edge is included as a control parameter. Thus the provenance of their model is different from ours but the spirit of their approach is similar to ours. They find their equations to have steady solutions (identified as ‘L’ and ‘H’ confinement modes), and by varying the energy input, transitions between these states are obtained. The shear flow, which we do not include, is responsible for the transition being similar to a first or second order phase transition. With sufficient energy, the H mode becomes unstable and bifurcates to a limit-cycle which shows periodic oscillations characteristic of ELMs. Of the differences between their work and ours, there is one which seems to merit comment. Their study makes no use of the inductive electric field. In our case, such a field is eliminated by the use of Faraday’s equation, thus leading to magnetic turbulence as one of our variables. It is instructive to note that recently<sup>16</sup> it has been found experimentally that even in regions where flow shear stabilization reduces *ion energy* and particle transport to near-neoclassical values, the electron thermal diffusivity can be high. This is suggestive that magnetic turbulence-dependent losses are probably important in determining the course of electron pressure evolution and micro-instabilities driven by it.

A general point worthy of some discussion is the fact that in the limit when the ‘neoclassical losses’, the coupling between the coherent mode and the turbulence, and the losses due to the pressure fluctuations from the time-averaged pressure are all neglected (ie weakly driven, but still a *nonlinear*, collisionless system), we obtain an exact conservation law<sup>2</sup> which leads to periodic solutions expressible in terms of elliptic functions, with the amplitude arbitrary. It is a function of the constant of the motion, which itself is not determined within the approximated model, but must be specified as an initial condition. This is due to a symmetry property of the dynamical equations in the above mentioned limit which actually corresponds to the fact that the  $Z$  and  $W$  equations are then transformable into a Hamiltonian system in a two-dimensional phase space. This ‘hidden symmetry’ is *spontaneously broken* by both the neglected nonlinear terms (ie those in the energy equation and the coupling terms relating to the coherent mode), and, more obviously, by the  $\kappa$  terms. We speculate that the fact that one observes, in certain conditions, rather regular, periodic relaxation phenomena in a highly turbulent, driven-dissipative system such as a tokamak may be a reflection of this spontaneously broken hidden symmetry of the equations of plasma physics. It is of interest to note in this context that in the paper of Sugama and Horton<sup>10</sup> the authors find that their conservation law leads only to growth.



Turning to the work of Diamond *et al*<sup>8</sup>, they too have set up a self-consistent model of the L-H transition. Their model consists of three coupled equations for the characteristic variables, density fluctuation level, average poloidal shear flow and the pressure gradient. The equations again exhibit stationary solutions corresponding to the L and H modes. The transition occurs when the turbulence drive is large enough to overcome the damping of the  $\mathbf{E} \times \mathbf{B}$  flow; this leads to a power threshold for the transition. Unlike our model, perhaps surprisingly for a three degree-of-freedom system, neither of the above two models reveal chaotic (intermittent or otherwise) solutions, ‘compound’ sawteeth/ELMs and solutions which seem to resemble ‘monsters’. Current thinking on the  $\mathbf{E} \times \mathbf{B}$  stabilization<sup>15</sup> tends to favour *turbulently* generated localized ‘zonal flows’ which serve to control the very turbulence that generates them. In simple low dimensional models, this idea would translate itself into the inclusion of terms like  $\phi(W)$  which effectively turn a *linear* drive into a nonlinear instability with weaker growth. As has been mentioned earlier, the nonlinear damping term on the *coherent* mode can indeed be thought of as an embodiment of this idea. Indeed, it is clear that some such mechanism is needed to explain why a linear mode with a relatively fast growth rate like the  $m = n = 1$  resistive internal kink is *not* unstable during the ramp.

## 6. Conclusions

In this paper, our purpose has been to extend a previously developed nonlinear dynamical model of sawteeth in tokamaks to include the possible effects of a single coherent mode. The physical principles which lie at the foundations of the model are rather general and would be expected to apply to a variety of relaxation oscillations found experimentally in a tokamak. Taking a particular spatial region, the pressure ( $Z$ ) (or a measure of pressure or temperature gradient) is evolved by balancing the applied source (assumed fixed) against both turbulent and non-turbulent losses. The turbulence intensity ( $W$ , analogous to Kolmogorov’s  $k$  in his  $k - \epsilon$  model) is driven in the first instance by the pressure and interacts in a model-dependent manner with the heat-flux as well as the coherent mode amplitude ( $X$ ). The latter is also driven by pressure but damped by both turbulent and neoclassical effects in a nonlinear sense (as in Landau-Stuart theory). We then show that these ingredients are sufficient to allow a rich variety of dynamical behaviour, including steady (ie sawtooth or ELM-free states), periodic, quasi-periodic, compound periodic, chaotic, ‘bursty’ chaotic and ‘monster-like’ solutions.

We have concentrated on the qualitative dynamical aspects and refrained from detailed model comparisons with experiment, since inevitably this leads to choosing parameters semi-empirically<sup>8, 10</sup>. The model shows that the most basic tokamak concepts (pressure or temperature-gradient drive, anomalous losses, nonlinear saturation by microinstability generation) are sufficient to qualitatively reproduce the dynamical characteristics of a range of plasma phenomena. This suggests that it should be possible to abstract from more detailed dynamical descriptions of tokamak plasmas the essential ingredients of relaxation oscillations, which appear to be fundamentally nonlinear in character.

Finally, we observe that there appear to be some deep-seated analogies between sawteeth and ELMing behaviour in tokamaks (and possibly also with fishbones and similar fast-particle-driven oscillations involving velocity space effects). This may have to do with



the fact that the linear drive of the equilibrium free energy (manifested either through pressure, current or temperature gradients) is nonlinearly coupled to turbulent transport, and both are in turn linked to some specific, macroscopic coherent mode (ie the  $m = 1$  in the case of sawteeth and edge ballooning/peeling modes for ELMs). The present model (along with its predecessors) sets out to abstract the essential features of this fundamentally nonlinear coupling with a view to isolating the crucial features. It is of interest that, although other models<sup>8, 10, 9</sup> differ from the present one in physical basis and specific features and achieve different aims, there is a certain invariant structure to all of them which points towards a model-independent description of relaxation phenomena mediated by turbulence in tokamak plasmas. In view of the fact that even such grossly oversimplified dynamical systems can exhibit a remarkably rich array of states and bifurcations, the complexity and range of relaxation oscillations and bifurcation behaviour observed in tokamak experiments should not be too surprising.

### Acknowledgements

The authors thank Dr. J.W. Connor for many useful suggestions. This work was funded jointly by the UK Dept. of Trade and Industry and Euratom.

### References

- <sup>1</sup> F.A. Haas and A. Thyagaraja, *Physics of Fluids B* **3**, 3388 (1991).
- <sup>2</sup> F.A. Haas F.A. and A. Thyagaraja , *Europhys. Lett.* **19** (4), 285 (1992).
- <sup>3</sup> F.A. Haas and A. Thyagaraja, *Plasma Phys. Control. Fusion* **37**, 415 (1995).
- <sup>4</sup> F.A. Haas and A. Thyagaraja, *Fusion Technology* **31**, 1 (1997).
- <sup>5</sup> A. Thyagaraja and F.A. Haas, *Physics of Fluids B* **5**, 3252 (1993)
- <sup>6</sup> L. Chen, R.B. White and M.N. Rosenbluth, *Phys. Rev. Lett.* **52**, 1122 (1984).
- <sup>7</sup> B.A. Carreras , P.H. Diamond , Y-M. Liang , V. Lebedev and D. Newman , *Plasma Phys and Contr. Fusion* **36**, A93 (1994).
- <sup>8</sup> P.H. Diamond , Y-M. Liang, B.A. Carreras, P.W. Terry, *Phys. Rev. Lett.* **72**, 2565 (1994).
- <sup>9</sup> S-I. Itoh , K. Itoh, A. Fukuyama , Y. Miura and the JFT-2M Group, *Phys. Rev. Lett.* **67**, 2485 (1991).
- <sup>10</sup> H. Sugama and W. Horton, *Plasma Phys. Control. Fusion* **37**, 345 (1995).
- <sup>11</sup> A.Y. Aydemir, J.C. Wiley and D.W. Ross, *Phys. Fluids B* **1**, 774 (1989).
- <sup>12</sup> E.N. Lorenz, *J. Atmos. Sci.* **20**, 130 (1963).

- <sup>13</sup> M.N. Bussac, R. Pellat, D. Edery and J.L. Soule, Phys. Rev. Lett. **35**, 1635 (1975).
- <sup>14</sup> J.W. Connor, Plasma Phys. Control. Fusion **40**, 531 (1998).
- <sup>15</sup> K.H. Burrell, Science **281**, 1816 (1998).
- <sup>16</sup> M.C. Zarnstorff, Bulletin of the Amer. Phys. Soc.(APS), 40th Annual Meeting of the Division of Plasma Physics (New Orleans), **43**, No. 8, 1635 (1998).

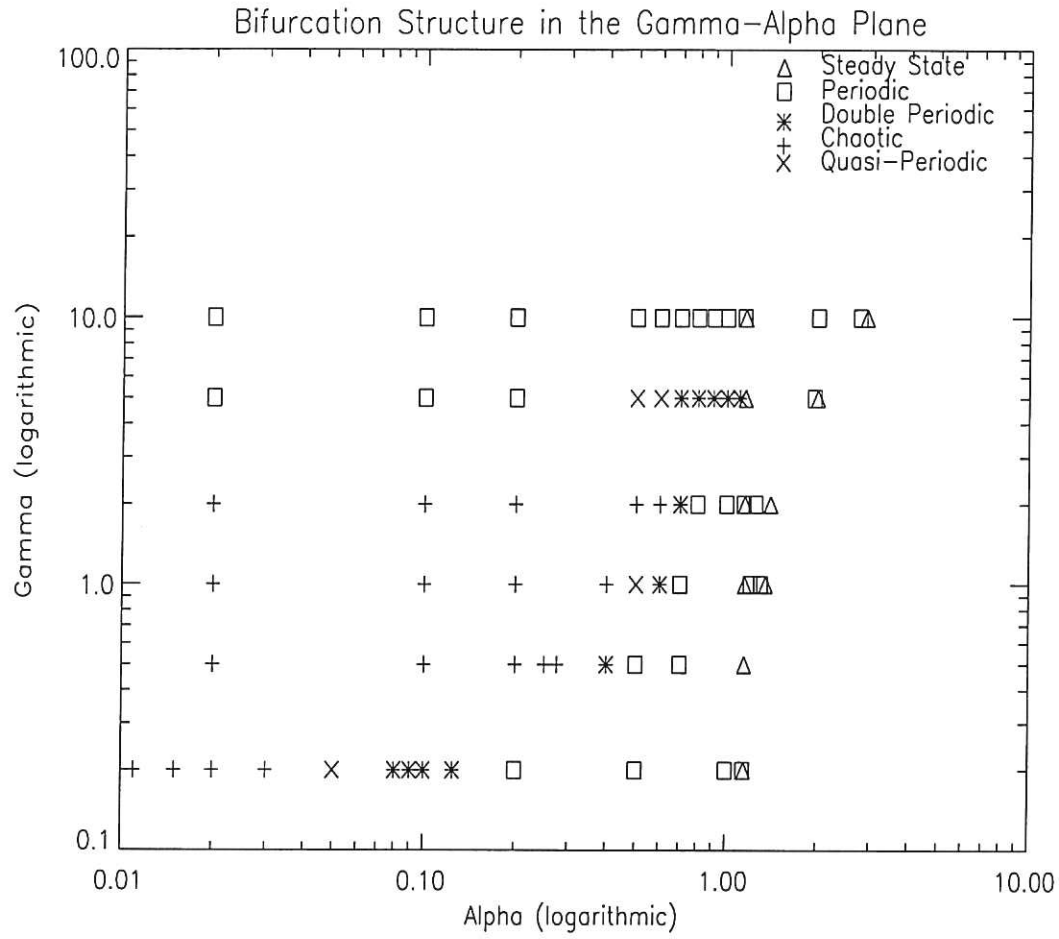


Fig. 1: Bifurcation Structure of System for  
 $\Lambda = 100, \kappa = 0.1, X_c = 0.1, Z_c = 0.25$

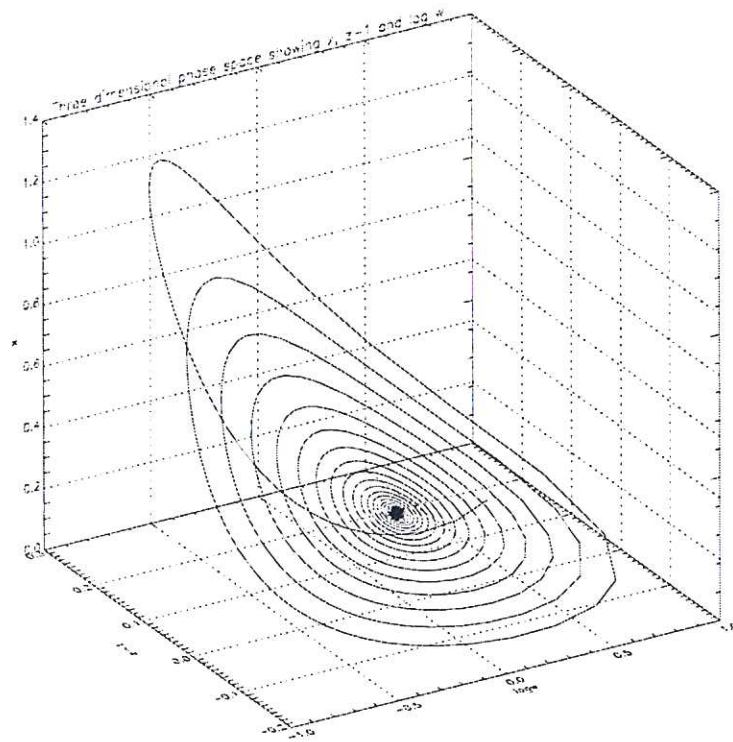


Fig. 2a: Phase Portrait of System for  
 $Z_0 = 1.05, W_0 = 0.9, X_0 = 0.6$ .

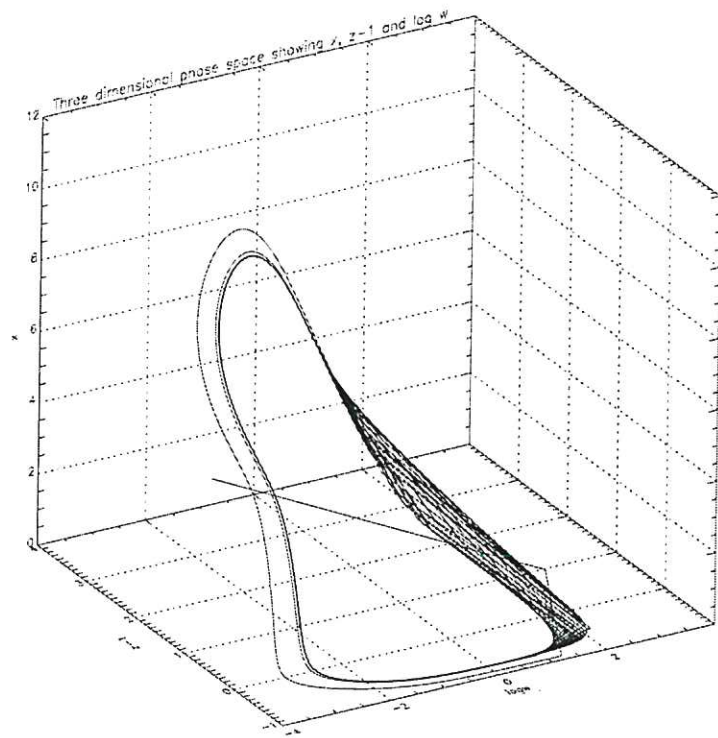


Fig. 2b: Phase Portrait of System for  
 $Z_0 = 5.0, W_0 = 0.1, X_0 = 0.6$ .



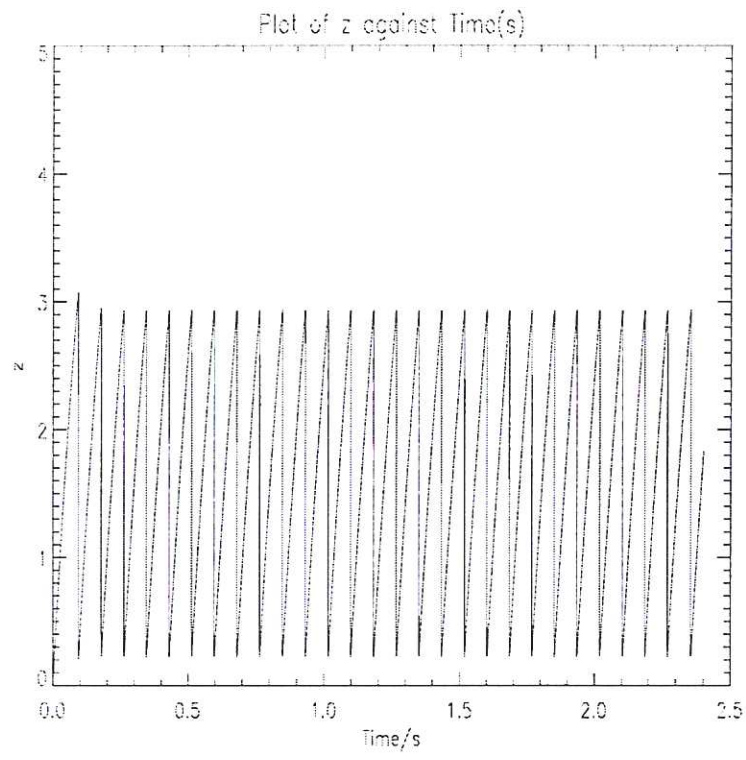


Fig. 2c:  $Z$  vs.  $t$  for  $Z_0 = 5.0, W_0 = 0.1, X_0 = 0.6$ .

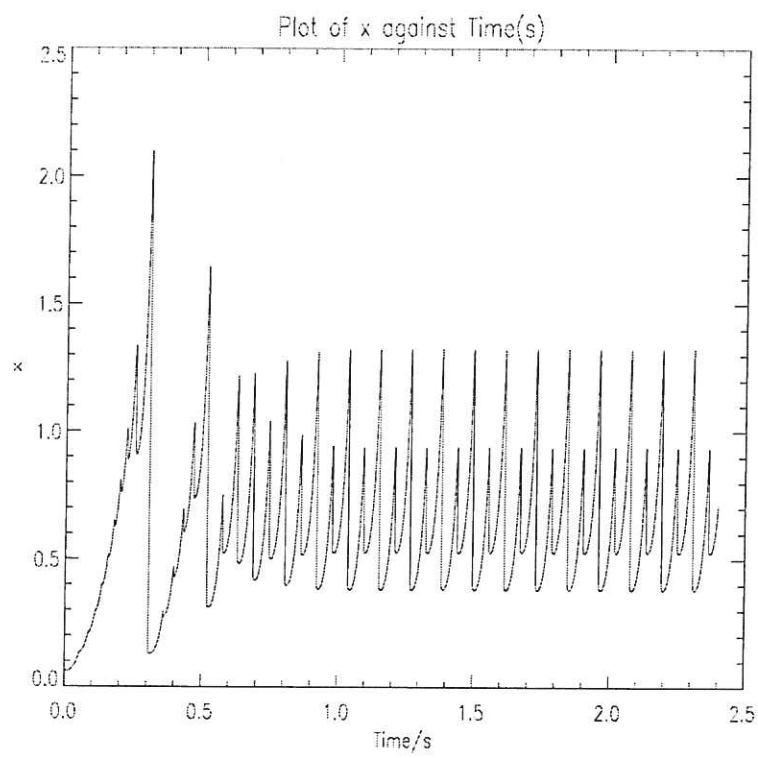


Fig. 3a:  $X$  vs.  $t$  for  $\alpha = 0.4, \gamma = 0.5$  showing ‘partial sawteeth’ or double periodicity

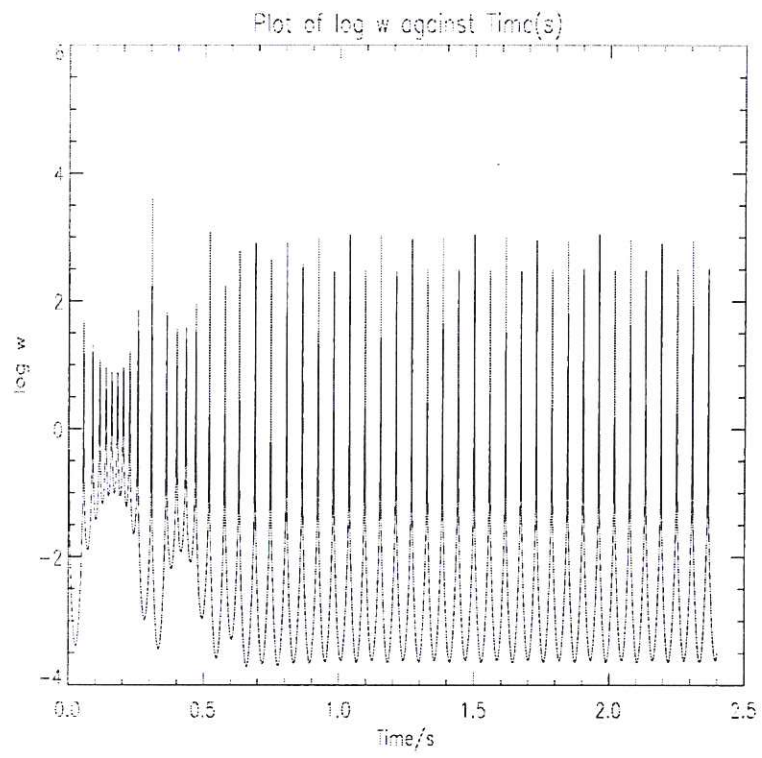


Fig. 3b:  $\log W$  vs.  $t$  for  $\alpha = 0.4, \gamma = 0.5$  showing ‘double periodicity’

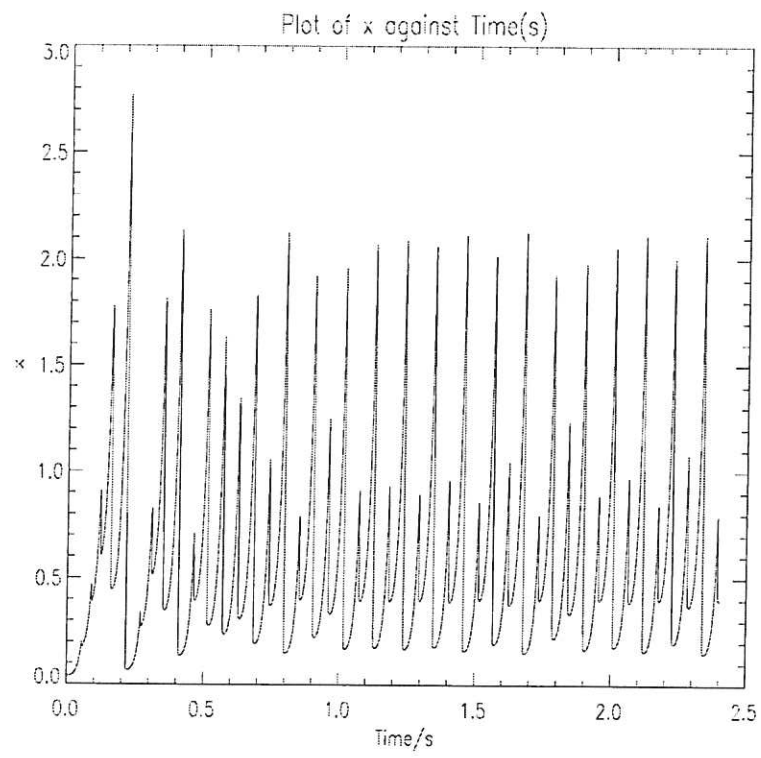


Fig. 4a:  $X$  vs.  $t$  for  $\alpha = 0.5, \gamma = 1.0$  showing 'quasi periodicity'

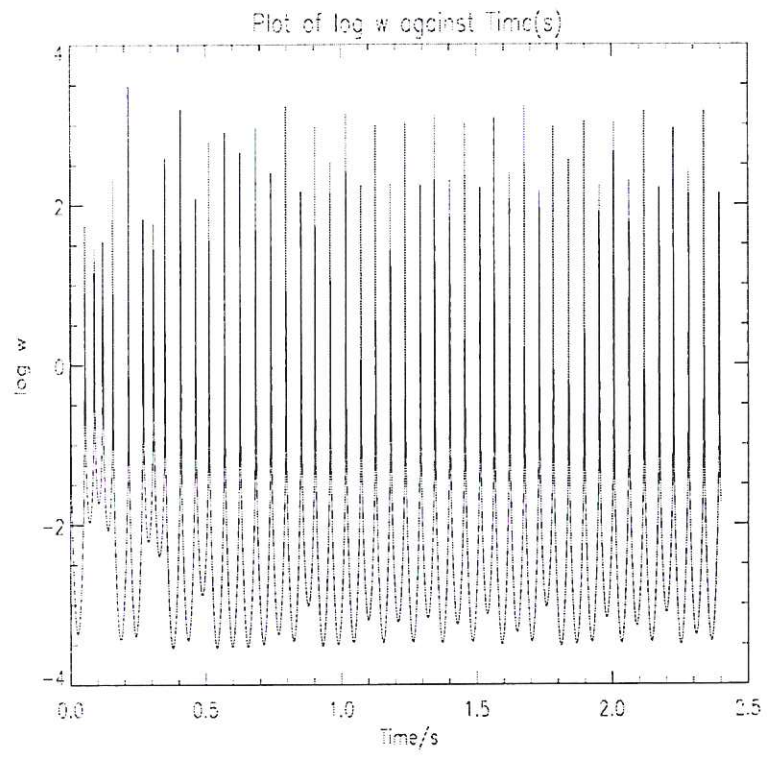


Fig. 4b:  $\log W$  vs.  $t$  for  $\alpha = 0.5, \gamma = 1.0$  showing ‘quasi periodicity’



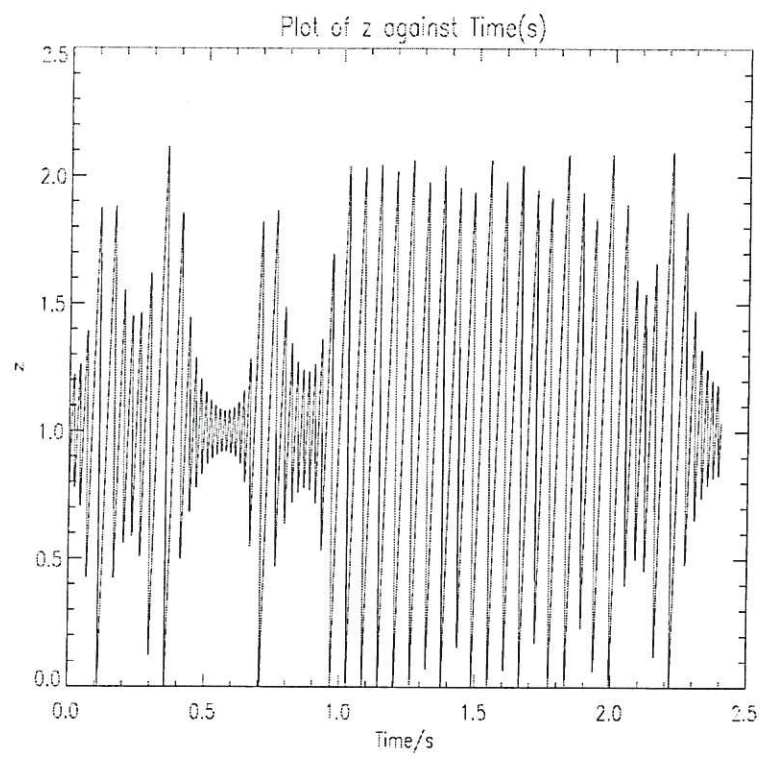


Fig. 5a:  $Z$  vs.  $t$  for  $\alpha = 0.25, \gamma = 0.5$  showing 'chaotic' sawteeth

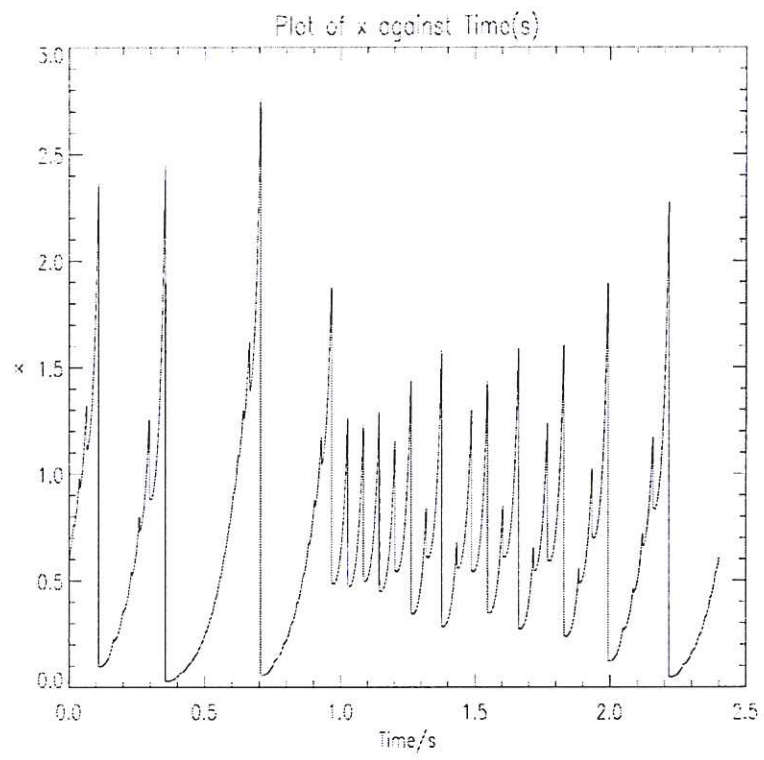


Fig. 5b:  $X$  vs.  $t$  for  $\alpha = 0.25, \gamma = 0.5$  showing 'chaotic' sawteeth

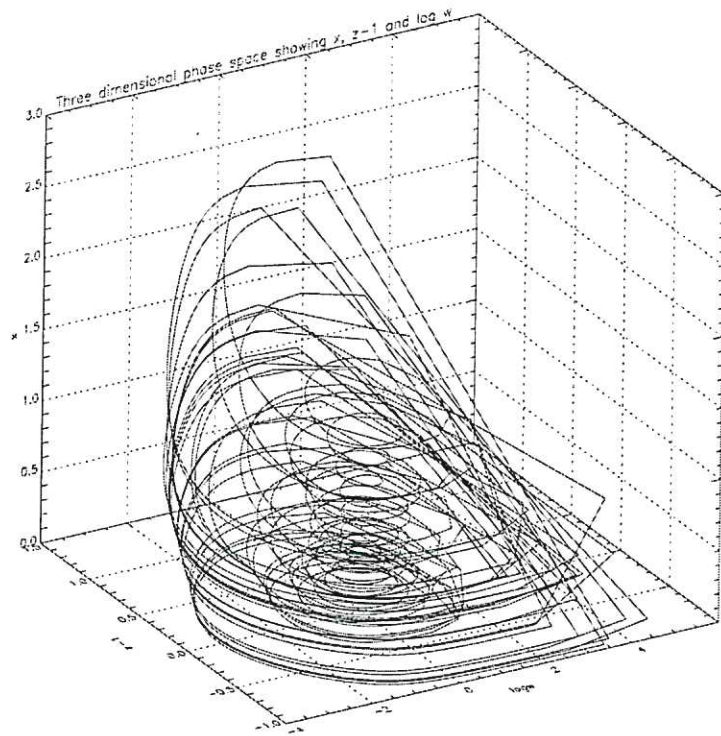


Fig. 5c: Three dimensional phase portrait (  $\alpha = 0.25, \gamma = 0.5$  )  
showing 'strange attractor'



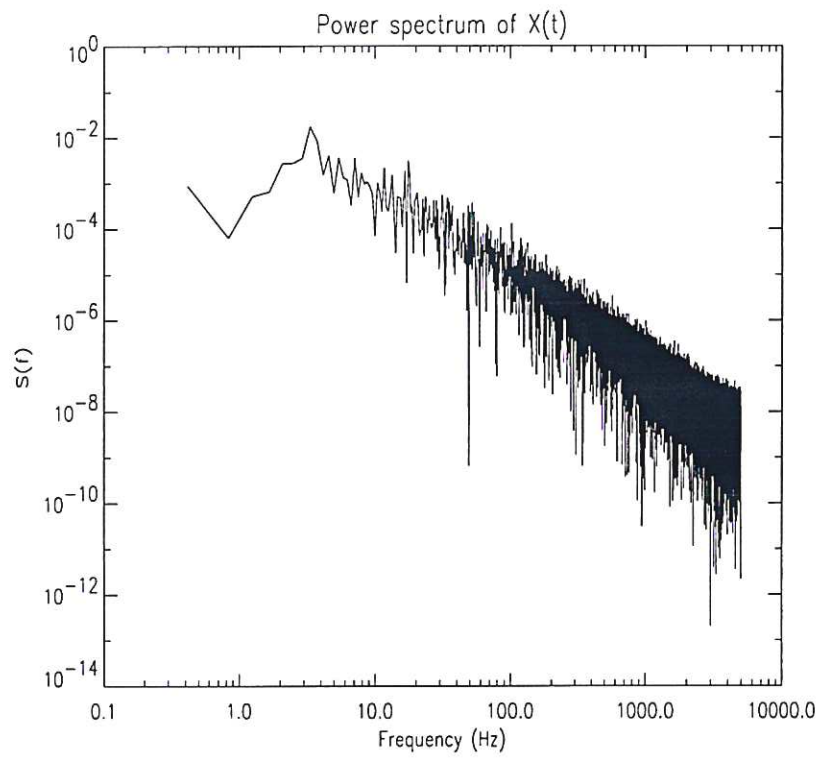


Fig. 5d: Frequency power spectrum of  $X$  in the chaotic case (  $\alpha = 0.25, \gamma = 0.5$  ). Note broad ‘incoherent’ component at high frequencies in addition to a few sharp ‘line’ spectra indicating coherent components.

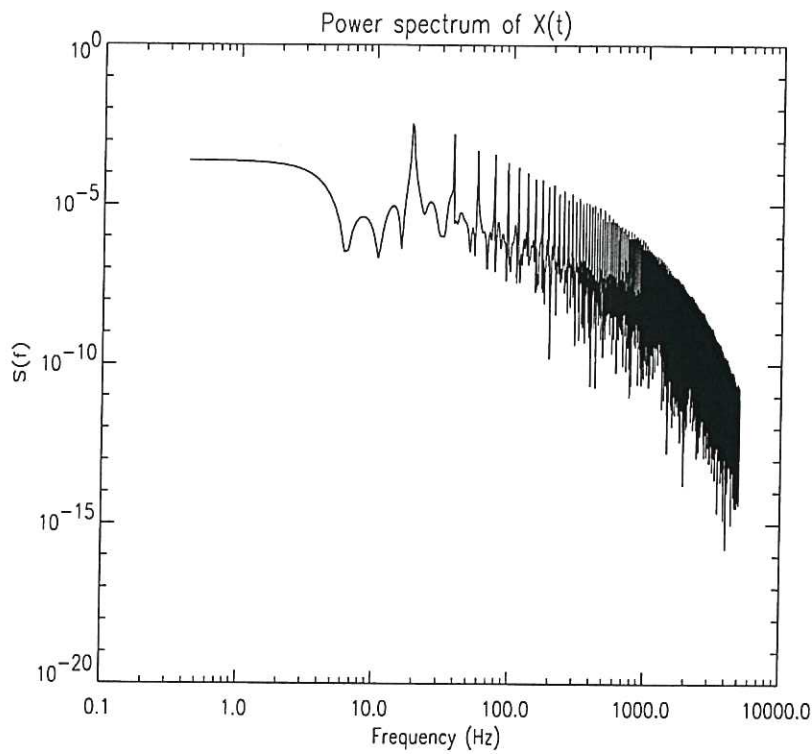


Fig. 5e: Frequency power spectrum of  $X$  in a periodic case ( $\alpha = 0.8, \gamma = 0.5$ ). Note the sharp coherent lines (essentially harmonics of the fundamental sawtooth frequency) and exponential decay of power at high frequency, in contrast to the power law decay of the chaotic spectrum in Fig.5d.

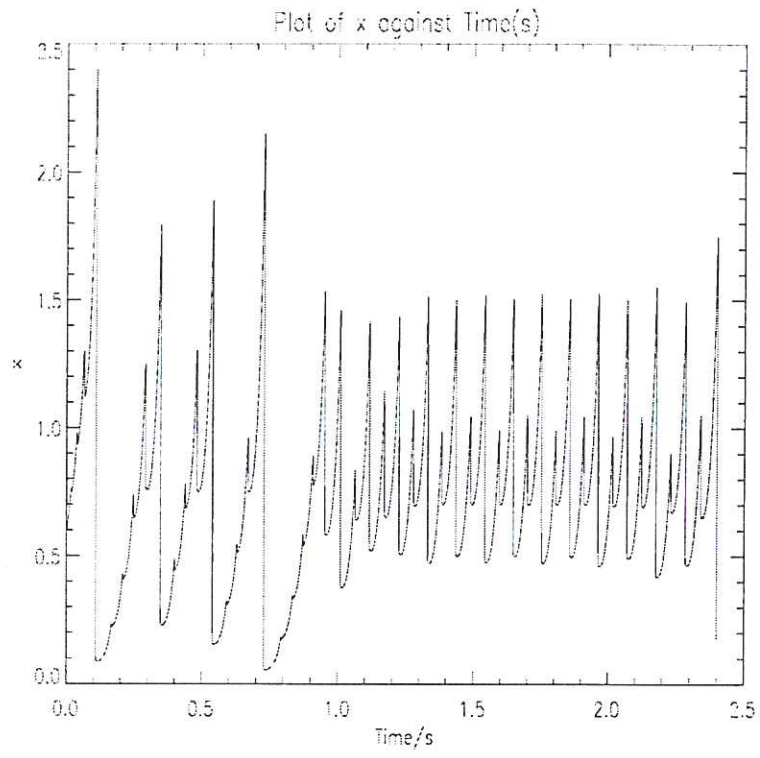


Fig. 6a:  $X$  vs.  $t$  for  $\alpha = 0.25, \gamma = 0.5$  illustrating ‘dynamic stabilization’ of chaos by a periodic, small amplitude external perturbation.



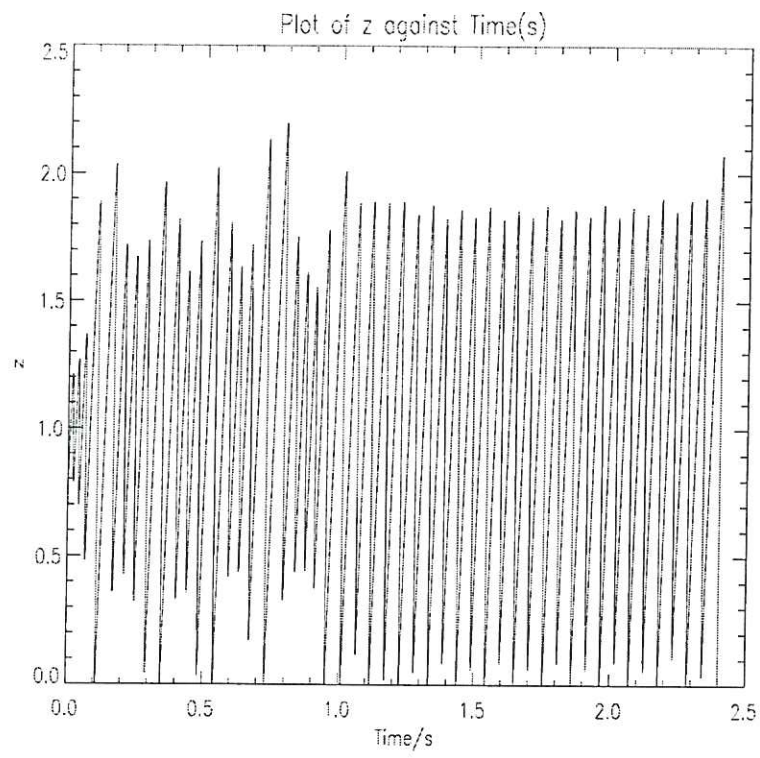


Fig. 6b:  $Z$  vs.  $t$  for  $\alpha = 0.25, \gamma = 0.5$  illustrating 'dynamic stabilization' of chaos by a periodic, small amplitude external perturbation.

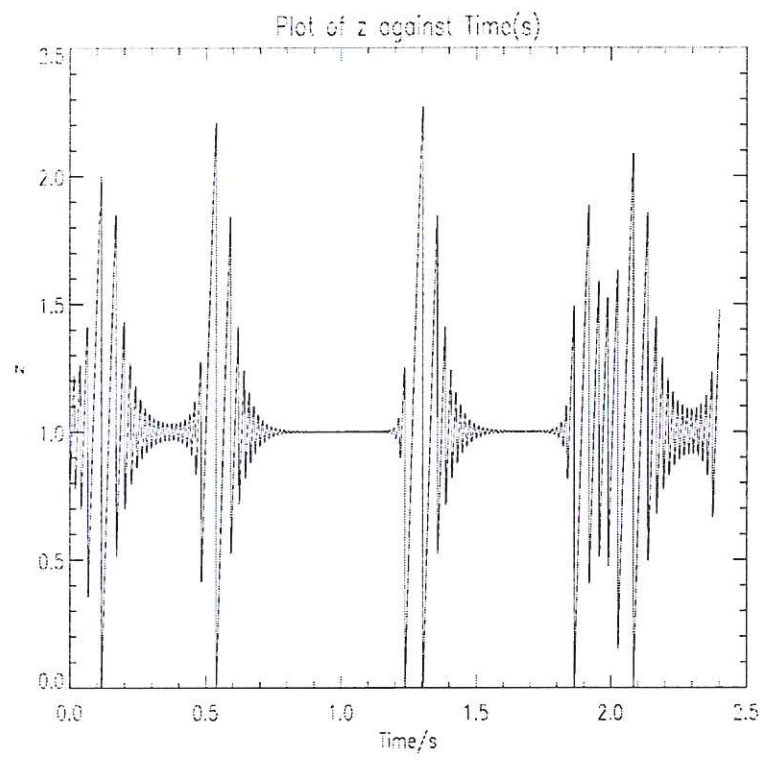


Fig. 7a:  $Z$  vs.  $t$  for  $\alpha = 0.2, \gamma = 0.5$  illustrating ‘bursty chaos’.

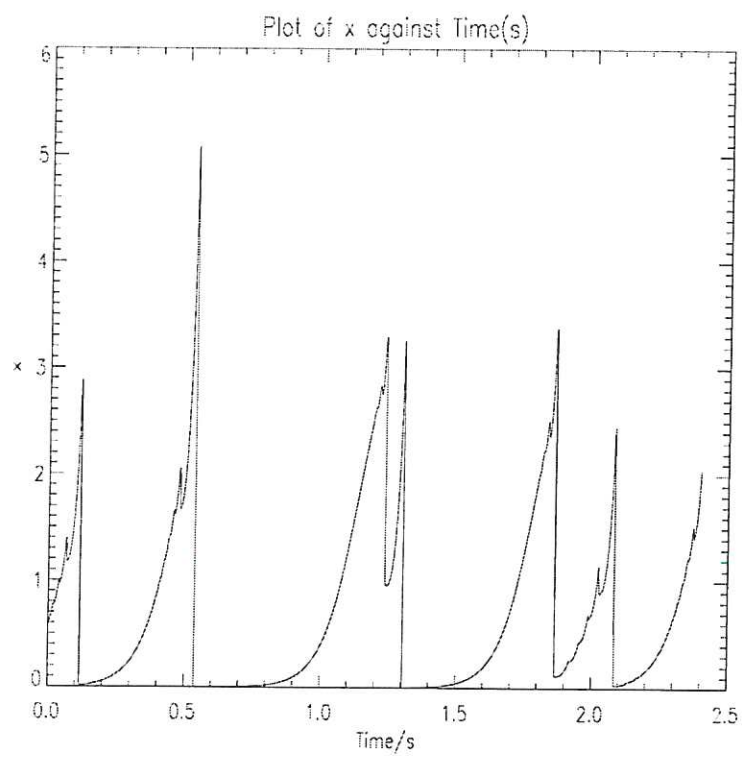


Fig. 7b:  $X$  vs.  $t$  for  $\alpha = 0.2, \gamma = 0.5$  illustrating 'bursty chaos'



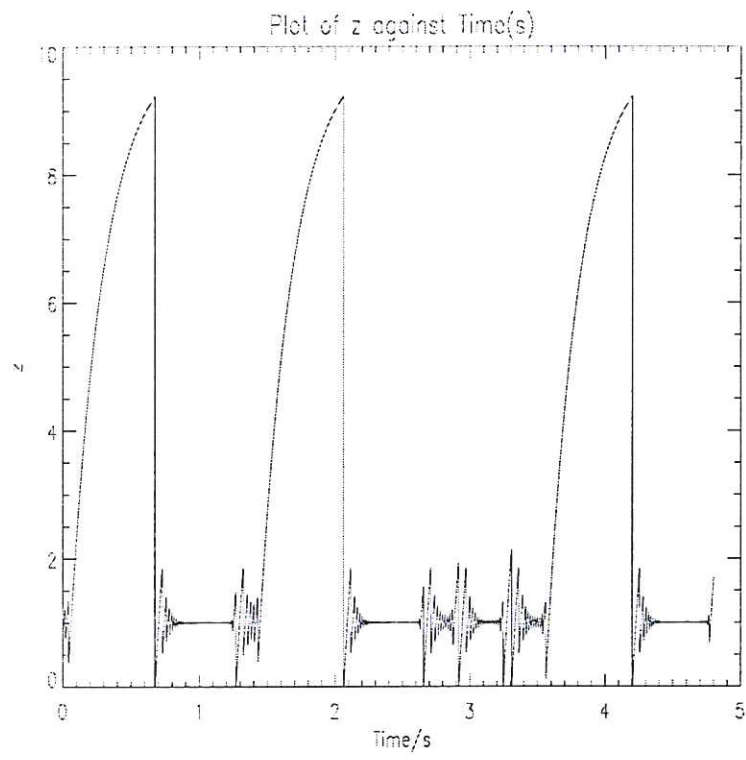


Fig. 8a:  $Z$  vs.  $t$  for  $\alpha = 0.2, \gamma = 1$  illustrating ‘intermittent monsters’.

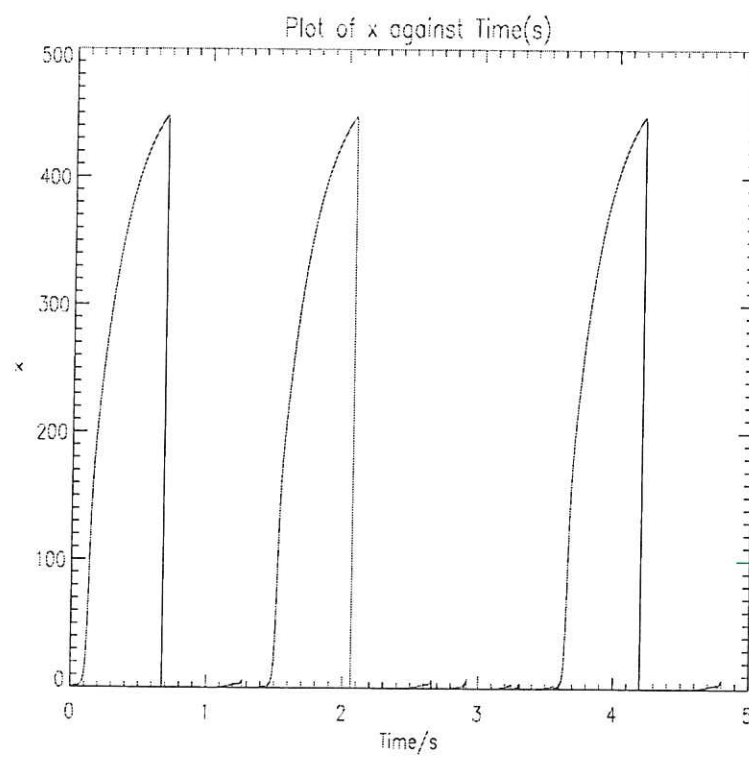


Fig. 8b:  $X$  vs.  $t$  for  $\alpha = 0.2, \gamma = 1$  illustrating 'intermittent monsters'

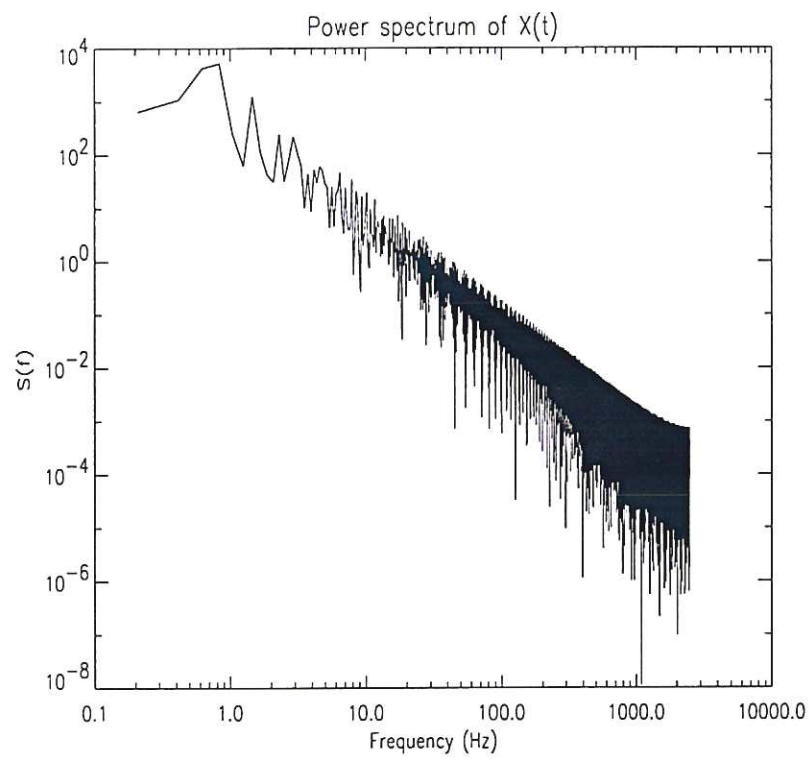


Fig. 8c: Fourier Power spectrum of  $X$  for  $\alpha = 0.2, \gamma = 1$  of the ‘monster’.



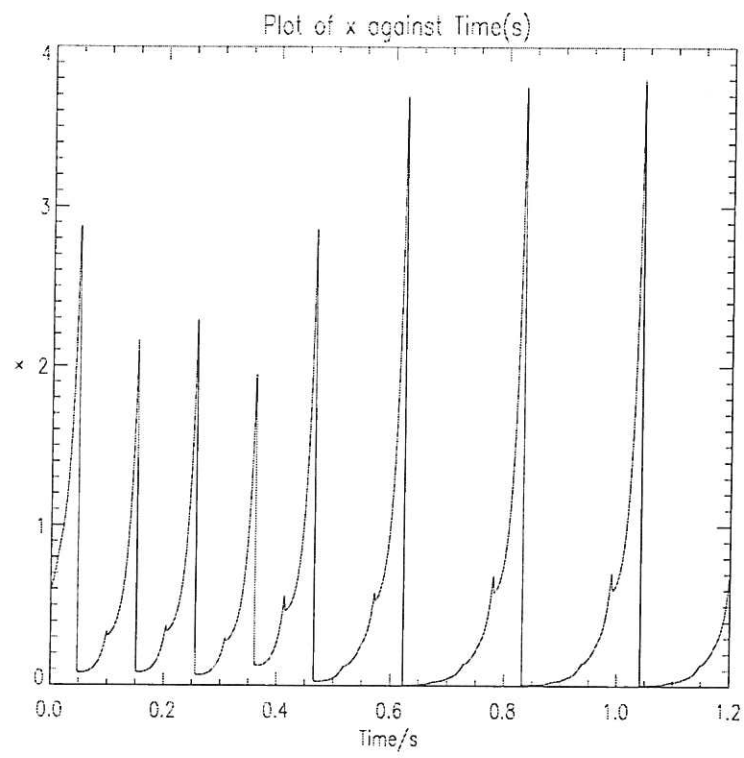


Fig. 9a:  $X$  vs.  $t$  for  $\alpha = 0.2, \gamma = 1$  illustrating dynamic stabilization of monsters.

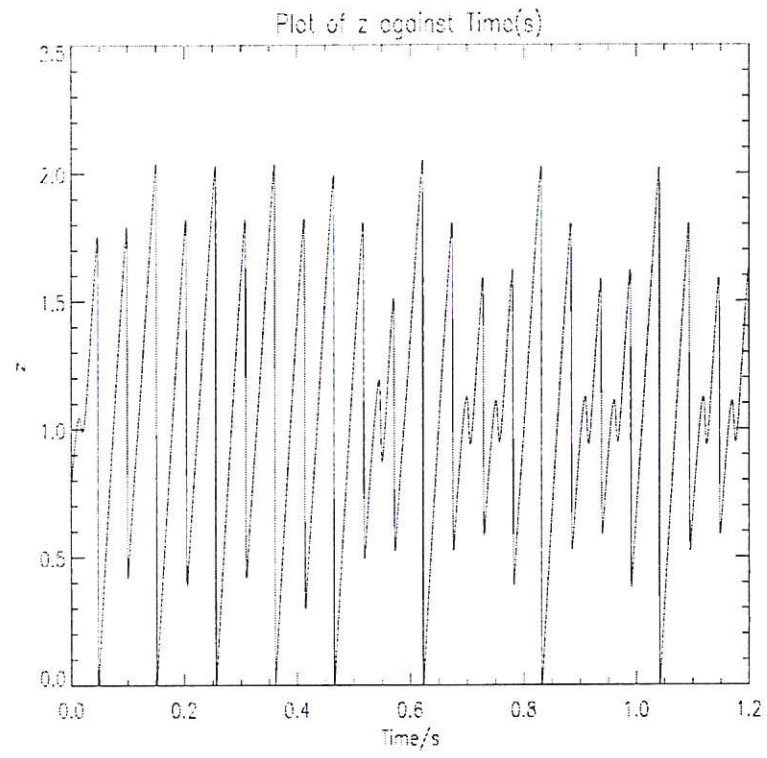


Fig. 9b:  $Z$  vs.  $t$  for  $\alpha = 0.2, \gamma = 1$  illustrating dynamic stabilization of monsters.

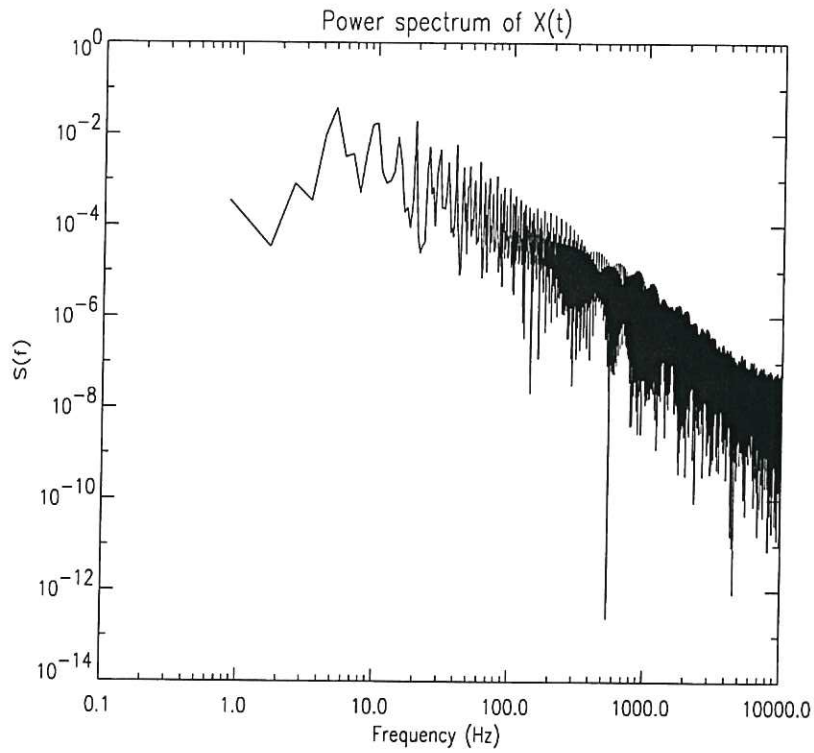


Fig. 9c: Fourier Power spectrum of  $X$  for  $\alpha = 0.2, \gamma = 1$  of the dynamically stabilized 'monster'. The applied perturbation frequency is 120 Hz. Compare with Fig.8c for the unstabilized monster.

